Apoferritin fibers: a new template for 1D fluorescent hybrid nanostructures†

Rocío Jurado,[a] Fabio Castello,[b] Patricia Bondia,[c] Santiago Casado,[c] Cristina Flors,[c] Rafael Cuesta,[d] José M. Domínguez-Vera,[a] Angel Orte*[b] and Natividad Gálvez*[a]

Recently, research in the field of protein amyloid fibers has gained great attention due to the use of these materials as nanoscale templates for the construction of functional hybrid materials. The formation of apoferritin amyloid-like protein fibers is demonstrated herein for the first time. The morphology, size and stiffness of these one-dimensional structures are comparable to the fibers formed by β-lactoglobulin, a protein frequently used as a model in the study of amyloid-like fibrillar proteins. Nanometer-sized globular apoferritin is capable of self-assembling to form 1D micrometer-sized structures after being subjected to a heating process. Depending on the experimental conditions, fibers with different morphologies and sizes are obtained. The wire-like protein structure is rich in functional groups and allows chemical functionalization with diverse quantum dots (QD), as well as with different Alexa Fluor (AF) dyes, leading to hybrid fluorescent fibers with variable emission wavelengths, from green to near infrared, depending on the QD and AFs coupled. For fibers containing the pair AF488 and AF647, efficient fluorescence energy transfer from the covalently coupled donor (AF488) to acceptor tags (AF647) takes place. Apoferritin fibers are proposed here as a new promising template for obtaining hybrid functional materials.

Introduction

The structuring of zero-dimensional (0D) nanoparticles has great interest in basic and applied research because they provide a direct link between the nanoscale and macroscale worlds.[1–3] Therefore, building structures of growing complexity using nano-objects is becoming desired for inorganic nanostructures as the applications of these materials continue to expand.[4,5] One-dimensional (1D) nanoparticle assemblies are thought to improve the efficiencies of various electronic, optoelectronic, and/or magnetic devices.[6,7] Likewise, 1D structures can significantly help in the understanding of numerous biological processes.[8,9] The simplicity of superstructure assemblies, their multifunctionality, and structural versatility

[a]Department of Inorganic Chemistry, University of Granada, Avda. Fuentenueva, Granada, 18071, Spain. E-mail: ngalvez@ugr.es
[b]Department of Physical Chemistry, Faculty of Pharmacy, University of Granada, Granada, 18071, Spain. E-mail: angelort@ugr.es
[c]IMDEA Nanoscience, 9 Faraday, Madrid, 28049, Spain
[d]Department of Organic and Inorganic Chemistry, EPS Linares, University of Jaén, 28 Alfonso X El Sabio, Linares, 23700, Spain
†Electronic supplementary information (ESI) available: TEM images of ferritin protein fiber formation, and apoferritin after 18 days of heat treatment; FLIM-PIE technique details; fluorescence emission spectra of apoferritin and β-lactoglobulin fibers functionalized with different QDs. See DOI: 10.1039/c6nr01044j

represent interesting directions for future research in nanostructures.[10]

Of particular interest are materials that act as a bridge between the inorganic and biological worlds: bioinorganic hybrid materials. Biological systems have great flexibility and capacity for self-assembly, hence the interest in them for nanotechnology. Biomolecules such as DNA, peptides or proteins have been widely used for the synthesis of bioinorganic materials.[11–20] These hybrid nanomaterials find broad applications in biology, such as tissue engineering, drug delivery, bioimaging or biosensors, and in nanotechnology, as templates for the fabrication of metal nanowires and functional polymer nanotubes due to their unique anisotropic properties.[21,22]

Numerous natural proteins such as tubulin, fibrin or collagen, occur as fibrous nanostructures in biological organisms, whose singular properties relate to their specific biological functions. Amyloid-like fibers, either natural or synthetic, and self-assembling peptides are excellent templates for the production of 1D inorganic nanostructures.[23–26] Some strengths of these 1D structures are: rigid structures with high mechanical strength, comparable in specific stiffness to spider silk and steel,[27–29] easy preparation from available proteins, and control over growth to obtain a variety of structures and physical properties. A strong and important point is that rigid amyloid fibers have rich and diverse surface functional groups on which other components with desirable functionalities can

easily be built with nanoprecision.[30] A last but not least advantage of protein fibers is that size diameters are homogeneous, reproducible and easily tuned.

An example of fibers prepared from a globular protein is the case of β-lactoglobulin (Blg).[31] Mezzenga and colleagues have numerous and very appealing contributions on how β-lactoglobulin amyloid protein fibrils act as perfect templates to drive the synthesis of different inorganic materials (carbon nanotubes, TiO_2, magnetite, gold) to form hybrid nanowires.[32–36]

Our group, among others,[37] has several reports on the preparation of metallic 0D nanoparticles using the protein apoferritin as a template. Besides, we have shown up the capability of this protein to be functionalized using the lysine residues at the external shell, introducing a new physical property.[38,39]

Experimental section

Preparation of the apoferritin (APO) and β-lactoglobulin (Blg) stock solution proteins

Horse spleen apoferritin and Biopure bovine β-lactoglobulin proteins were purchased from Sigma-Aldrich. Apoferritin and β-lactoglobulin protein solutions (2 mL, 4 mg mL^{-1}) were purified by centrifugation (13 552 rcf, 15 min) and the supernatant was filtered through a 0.22 μm Millipore filter.

Influence of temperature, pH and incubation time on fiber formation

Purified protein solutions were adjusted to the appropriate pH (2 or 5, diluted HCl dissolved in Milli-Q water) before heat treatment (50 °C or 80 °C, glass tubes hermetically sealed) over incubation time periods of 5 min, 10 min, 20 min, 30 min, 40 min, 50 min, 1 h, 3 h, 12 h, 24 h, 48 h or 120 h. After heat treatment, glass tubes were cooled in an ice bath to quench the aggregation process. Samples were collected for TEM analysis.

Preparation of the dye-labelled fibril proteins

In a first step amyloid-like protein fibers were formed after the heat treatment of protein solutions at 80 °C and pH 2 for 12 hours. Later, the so-obtained fibril proteins were purified by ultrafiltration using VIVASPIN 6 with a molecular weight cut-off (MWCO) of 100 000 Da. Alexa Fluor succinimidyl ester derivatives (AF488, AF647) were purchased from Life Technologies. Solutions of protein fibers (2 mL) were prepared in aqueous solution pH 8.0 and incubated for 24 h with the corresponding fluorophore succinimidyl ester derivatives specifically, AF488 (tag1), AF647(tag2) or a mixture of both to obtain FRET samples in a 1 : 1 : 1 (protein : tag1 : tag2) stoichiometry. The resulting solutions were then exhaustively dialyzed for 3 days against several changes of distilled water.

Synthesis of fluorescent 1D hybrid QD-fibers

Amyloid-like protein fibers were prepared as described previously. Carboxyl-coated quantum dots (QD525, QD655,

QD800) were purchased from Life Technologies. 1-Ethyl-3-[3-dimethylaminopropyl]carbodiimide hydrochloride (EDC) was purchased from Sigma-Aldrich. 10 μL of a stock solution (10 mg mL^{-1}) of EDC in milli-Q water was mixed with a carboxyl-QD stock solution (20 μL, 8 μM) for 30 min at room temperature. A 2 mL APO and Blg protein fiber solution at pH 8.0 was added to this mixture and incubated for 24 h. Fluorescence emission and excitation spectra were recorded on a Cary Eclipse spectrofluorometer.

Correlative AFM and fluorescence imaging

Correlative imaging was performed with a JPK Nanowizard II AFM coupled to a Nikon Eclipse Ti inverted optical microscope, as previously described.[42] Samples were dried on glass and imaged in air with NSG30 cantilevers (NT-MDT). For fluorescence imaging, samples were excited at 488 nm with a Luxx laser (Omicron) and imaged onto an EMCCD camera (iXon Ultra 897, Andor Technology) through a 60× NA 1.49 oil immersion objective (Nikon).

Fluorescence lifetime imaging microscopy with pulsed interleaved excitation (FLIM-PIE) measurements

FLIM-PIE experiments of APOft and Blg were performed with a MicroTime 200 time-resolved fluorescence microscope (PicoQuant GmbH, Germany). We employed a dual-color pulsed interleaved excitation (PIE) scheme, with two spatially overlapped pulsed lasers, at 470 (LDH-P-C-470, PicoQuant) and 635 nm (LDH-P-635, PicoQuant). These settings permit the simultaneous collection in a single step of the donor FLIM image, the FRET image, and the directly excited acceptor fluorescence intensity image. For more experimental details, see the ESI.†

Electron microscopy study

Samples were prepared by placing a drop onto a carbon-coated Cu grid. Electron micrographs were taken with a LIBRA 120 PLUS microscope operating at 120 keV. HR-STEM, HAADF-STEM and EDX maps were obtained with a FEI TITAN G2 microscope.

Results and discussion

Formation of APO and Blg fibers

Apoferritin (APO), the empty ferritin protein resulting from iron oxide removal, is a globular protein composed of 24 polypeptide subunits (M_r 450 kDa) with a hollow aqueous cavity 8 nm in diameter where it can accommodate an iron oxide nanoparticle. Ferritin is the primary Fe storing protein in most living organisms.[40] It is remarkably stable to temperature and pH changes, as demonstrated by its stability up to 70 °C and over extreme pH values of 3–10.

TEM contrasted images of the two globular APO and Blg proteins are shown in Fig. 1. Native APO is a hollow protein shell with cubic symmetry. At neutral pH and room temperature (RT), APO shows the typical spherical mor-
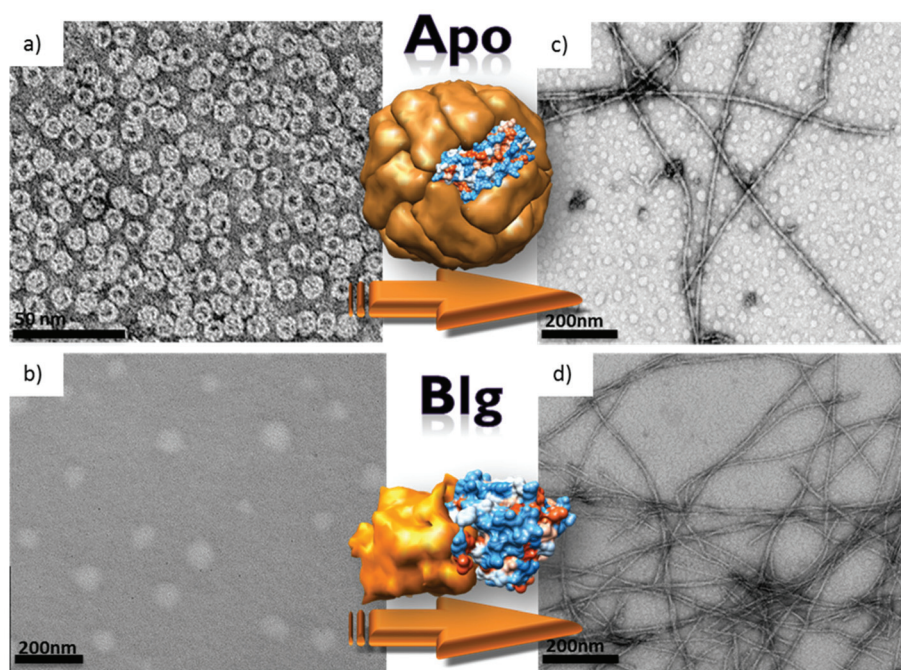
Fig. 1   TEM contrasted images of (a) the globular native APO protein at pH 7.4 and RT, (b) the globular Blg protein at pH 5 and 80 °C, (c) amyloid-like fibrillar APO at 80 °C, pH 2 and 24 h, (d) same as (c) for Blg.

phology with an average diameter of 12 nm (Fig. 1a). Under the same conditions of pH and temperature Blg forms dimers and a heat treatment at 80 °C and pH 5.0 is necessary for obtaining globular structures, in particular spherical aggregates with a size distribution centered at about 50–100 nm (Fig. 1b).[36] Blg is known to form well-structured fibrils when the temperature is increased above 70 °C under very acidic conditions (pH 2). Fig. 1c (APO) and 1d (Blg) show TEM images after heat treatment at 80 °C and pH 2 for 24 h. For the Blg protein, wire-like structures with an average diameter of 10 nm and several microns in length were observed, in agreement with previous reports.[36] Similar to Blg, the APO protein forms quite rigid (segments of 200–1000 nm, straight segments), rod-like fibers with diameters of 10 ± 2 nm. More flexible fibers were formed when the ferritin protein was subjected to the same heat treatment (see ESI, Fig. S1†). To optimize the synthesis of these APO protein nanowires we performed an exhaustive study varying the experimental conditions, which was followed by TEM.

Influence of temperature

The temperature dramatically influences the final 1D structure obtained (Fig. 2). More flexible and aggregated fibers, with bigger diameters of 20–30 nm, were formed when the temperature is decreased from 80 (Fig. 2a) to 50 °C (Fig. 2b). It should be pointed out that the Blg protein did not form fibers at 50 °C, but temperatures higher than 70 °C must be applied, as previously reported.[36]

Influence of pH

The influence of pH on the APO fiber formation is shown in Fig. 3. Four different stages of the APO amyloid-like fibril formation can be distinguished after a heat treatment at 50 °C in a weak acidic medium (pH 5). In Fig. 3a, it can be observed how the native APO protein forms aggregates while maintaining its globular structure. In Fig. 3b APO cages stick together and the process of fiber formation begins and accordingly, thick fibers of APO cages with diameters of 80–100 nm are observed. At this stage the globular native structure of APO, and even its inner cavity (a dark spot at the middle of the cage) can still be perfectly distinguished. In Fig. 3c, after a heat treatment of 40 min, the globular structure is barely observed since the fibrillar process goes on. In fact after 24 h of incubation time, Fig. 3d, fibers of 20–50 nm in diameter were formed. They were more aggregated, disordered and thicker than fibers formed at pH 2 and 50 °C (Fig. 2b). The native globular structure was lost in the final stage. Briefly, during the heating process at 50 °C and pH 5 the globular APO protein cages stick together and they arrange forming thick, aggregated and flexible fibers of around 20–50 nm. Under these experimental conditions (pH 5, 50 °C) the process of fiber formation occurs slowly, compared to that at 80 °C, which allowed us to monitor the system at 4 different stages of the fiber formation process. After 18 days, thinner fibers, but still flexible, were observed (see ESI, Fig. S2†), similar to the ones obtained at pH 5 and 80 °C after 24 h.

Whereas the Blg protein only forms fibers under very acidic conditions (pH 2) and high temperatures (80 °C), APO fibers can be obtained at lower temperatures (50 °C) and higher pH values (5).
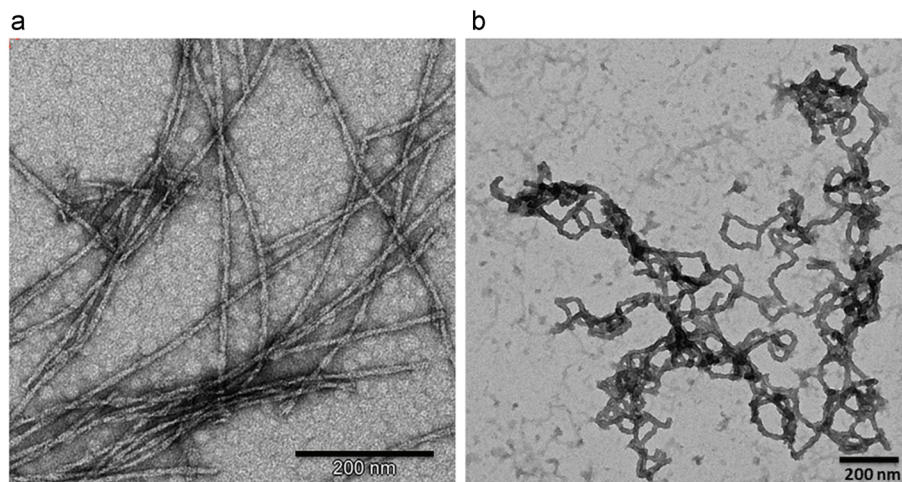
Fig. 2 TEM images of APO (a) heated at 80 °C and (b) 50 °C (pH 2 and 24 h of incubation time in both experiments).
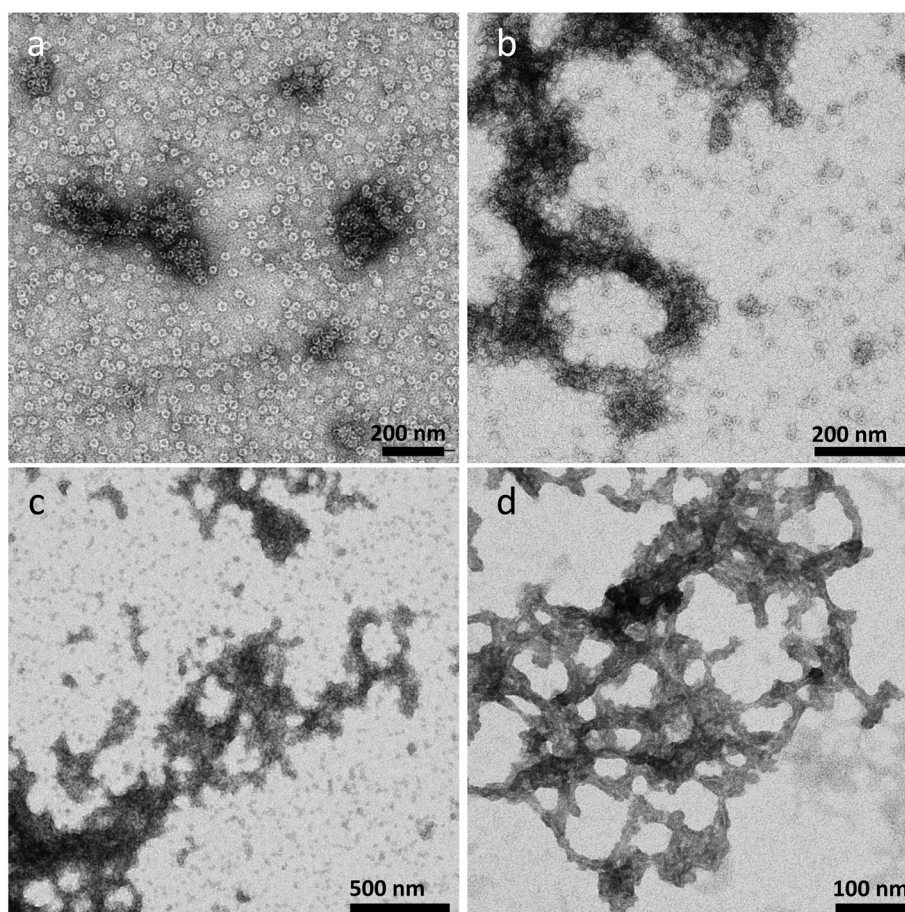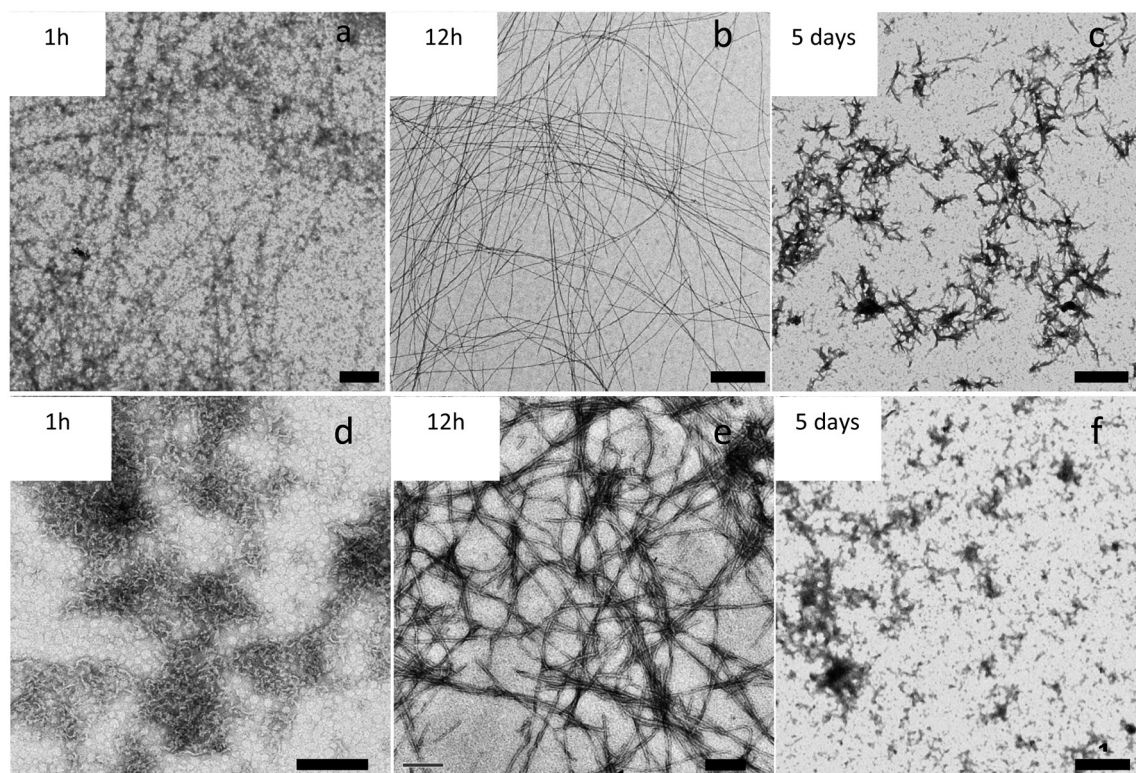

Fig. 3 TEM images of the APO protein heated at 50 °C and pH 5 for different incubation times. (a) 5 min, (b) 20 min, (c) 40 min and (d) 24 h.

Influence of incubation time

We also observed that incubation time is another key factor affecting the morphology of the fibers. Fig. 4 shows the

evolution with time of APO and Blg fibers while heating at 80 °C and pH 2. Large protein aggregates were formed after 1 h of treatment (Fig. 4a and b). Protein fibers were formed after 12 h of incubation time (Fig. 4c and d), remained until

Fig. 4 TEM images of APO and Blg heated at 80 °C and pH 2 for different incubation times. Upper row: the Blg protein incubated for (a) 1 h, (b) 12 h and (c) 5 days. Bottom row: the APO protein incubated for (d) 1 h, (e) 12 h and (f) 5 days. Scale bar lengths: 1 μm for (a), (b), (c) and (f); 200 nm for (d) and (e).

48 h and then started to break down. After 5 days (Fig. 4e and f) of heat treatment amyloid-like fibers were broken and only smaller protein aggregates could be observed.

After globally considering the influence of temperature, pH and incubation time, we conclude that pH 2, 80 °C and an incubation period between 12–24 h are the optimal synthetic conditions to form well-structured, wire-like fibers for APO proteins with long persistence lengths.

Dye-labelled fibril proteins

It is interesting to highlight that, as expected, once the fibers were formed, the APO protein lost its ability to store Fe, which reflects the dramatic changes occurring at channels and cavity sites in the protein structure in fibers with respect to the native form. At this point, we wondered if fibers would retain the ability to be functionalized externally exhibited by native apoferritin. Indeed, amyloid fibrils have rich and diverse surface functional groups. However, few reports have been published on the use of these reactive groups as a template for chemical functionalization.[17,19,30] In particular, the native APO protein contains lysine and cysteine residues on the external surface that can be used to covalently couple molecules or nanoparticles as our group and others have previously reported.[37–39]

Following the same approach we have covalently bound two Alexa Fluor dyes and three types of quantum dots (QDs) with diverse fluorescence emission to the APO fibers. The 1D
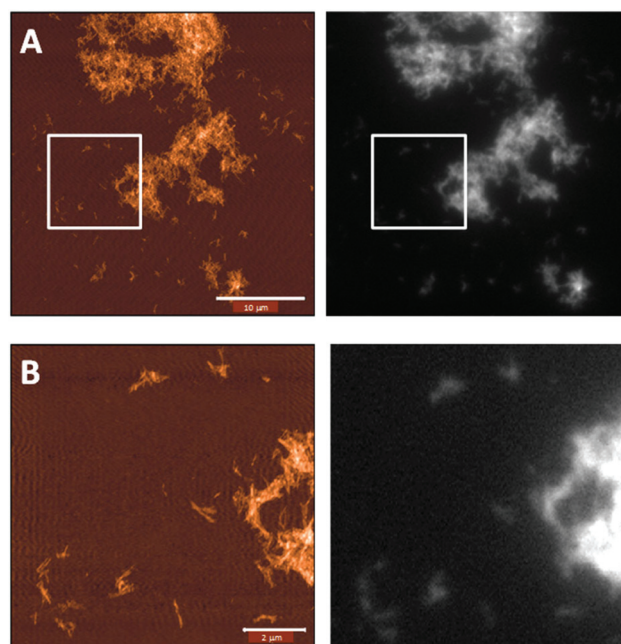
Fig. 5 Correlative AFM (left) and fluorescence imaging (right) of Blg fibers labeled with AF488 that confirms the attachment of the fluorophore to the fiber. B is the zoom of the white squared area in A.

bioinorganic hybrid nanostructures could find numerous applications, such as in the synthesis of inorganic nanowires that incorporate optical and electronic properties "à la carte".

AF dyes are intensely fluorescent, and their succinimidyl ester derivatives react with amine groups, giving rise to conjugate proteins with high photostability. AF488 and AF647 molecules were readily bound to the APO and Blg nanofibers by the formation of amide bonds. In this way, 1D fluorescent nanofibers were obtained. In a first experiment, APO and Blg fibers were reacted with only AF488 or AF647.

To confirm that the functionalization was successful, we imaged the fibers with correlative AFM and fluorescence microscopy. Indeed, Fig. 5 shows that the pattern in the fluorescence image matches that of the fibers in the AFM image.

Fluorescence lifetime imaging microscopy with pulsed interleaved excitation (FLIM-PIE) measurements

In order to obtain more information about the arrangement of the fibers, we focused on the FRET from AF488 (donors) to AF647 (acceptors) by observing the donor fluorescence lifetime using Fluorescence Lifetime Imaging Microscopy with pulsed interleaved excitation (FLIM-PIE). FLIM imaging allows

mapping the lifetime of the donor, τ_D, which depends on the FRET efficiency, and the PIE excitation scheme provides simultaneous dual-colour excitation for colocalization imaging of the donor and acceptor (see the ESI and Fig. S3† for details).[41] We performed FLIM-PIE experiments on APO and Blg, both in the native globular form (APO-globular and Blg-globular) and fibers (APO-fibers, Blg-fibers), labeled with both AF488 and AF647 (Fig. 6). In the FLIM analysis of the APO-fibers (Fig. 6a and b for representative images, and more images are collected in Fig. S4†), we distinguished two different populations: fibrillar structures characterized by high fluorescence intensity due to a high number of emitting dyes, and high FRET efficiency (τ_D distribution centered at 2.40 ± 0.01 ns, Fig. 6b,i); and small aggregates with less efficient FRET (τ_D distribution centered at 3.13 ± 0.02 ns, Fig. 6b,ii), which suggest a less organized conformation of these aggregates. In contrast, APO-globular exhibited a τ_D distribution centered at 3.53 ± 0.01 ns (Fig. 6b,iii), indicating a low-FRET. Similar results were obtained for Blg (Fig. 6c and d). Blg-fibers exhibited highly-fluorescent fibrillar structures, characterized by a τ_D centered at 3.06 ± 0.01 ns, coexisting with small aggregates (τ_D centered at 3.12 ± 0.01 ns). These small aggregates are different from
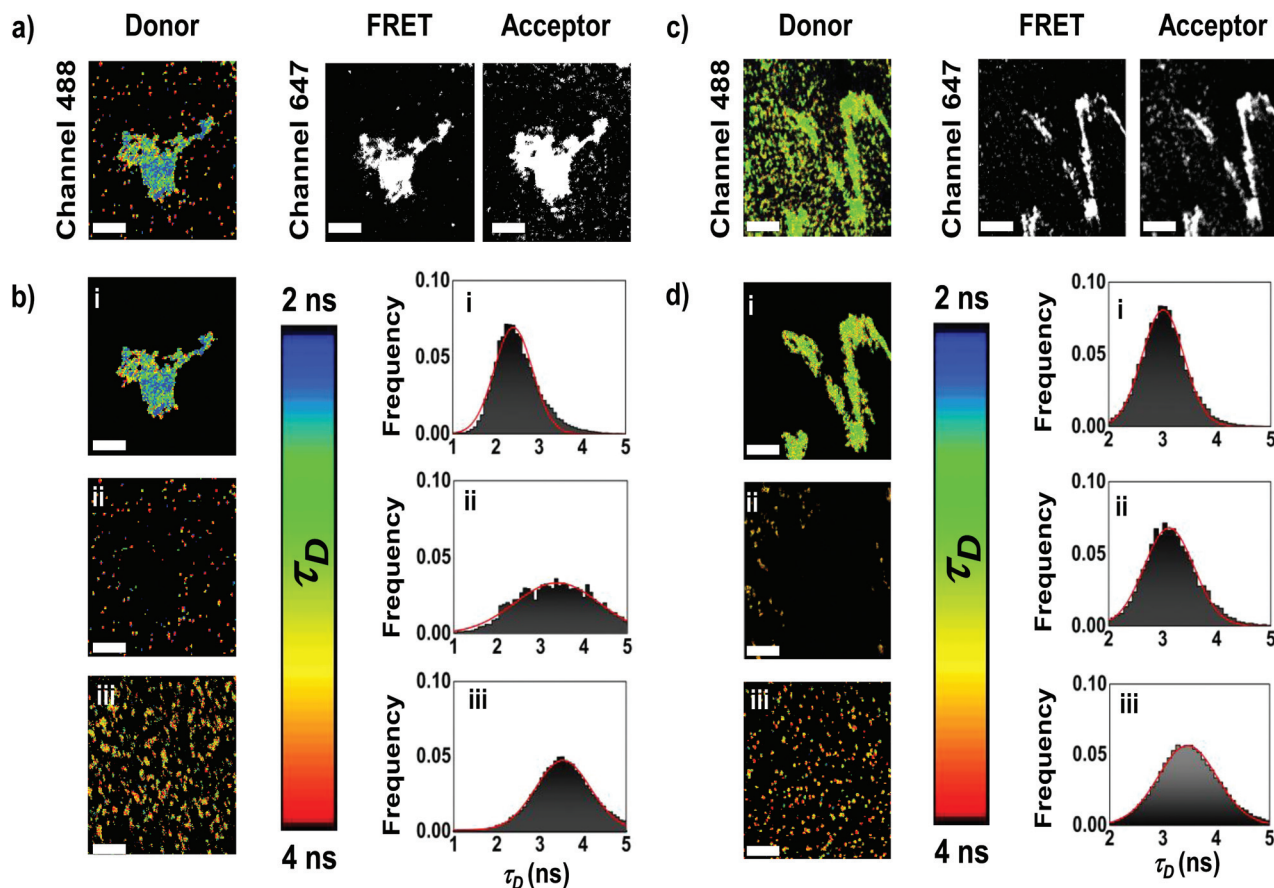
Fig. 6 FLIM-PIE experiments of APO and Blg, in fibers and globular forms tagged with both AF488 and AF647. Donor FLIM image, FRET and directly excited acceptor fluorescence images of APO-fibers (a) and Blg-fibers (c). The donor FLIM images and τ_D distributions of APO (b) and Blg (d) in fibrillar structures (i) and small aggregates (ii) are shown and compared with the globular forms (iii). The distributions were normalized by using events from 5 different images. White scale bars: 3.3 μm.
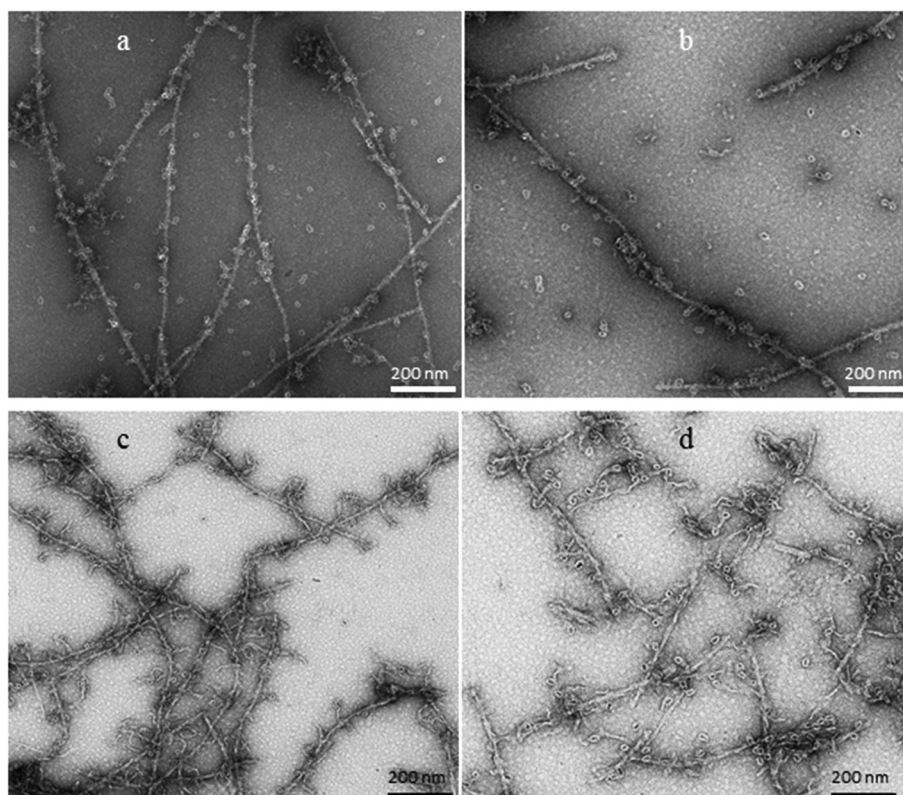
Fig. 7 HR-TEM images of (a) Blg-QD655, (b) Blg-QD800, (c) APO-QD655 and (d) APO-QD800 1D fluorescent hybrid fibers.
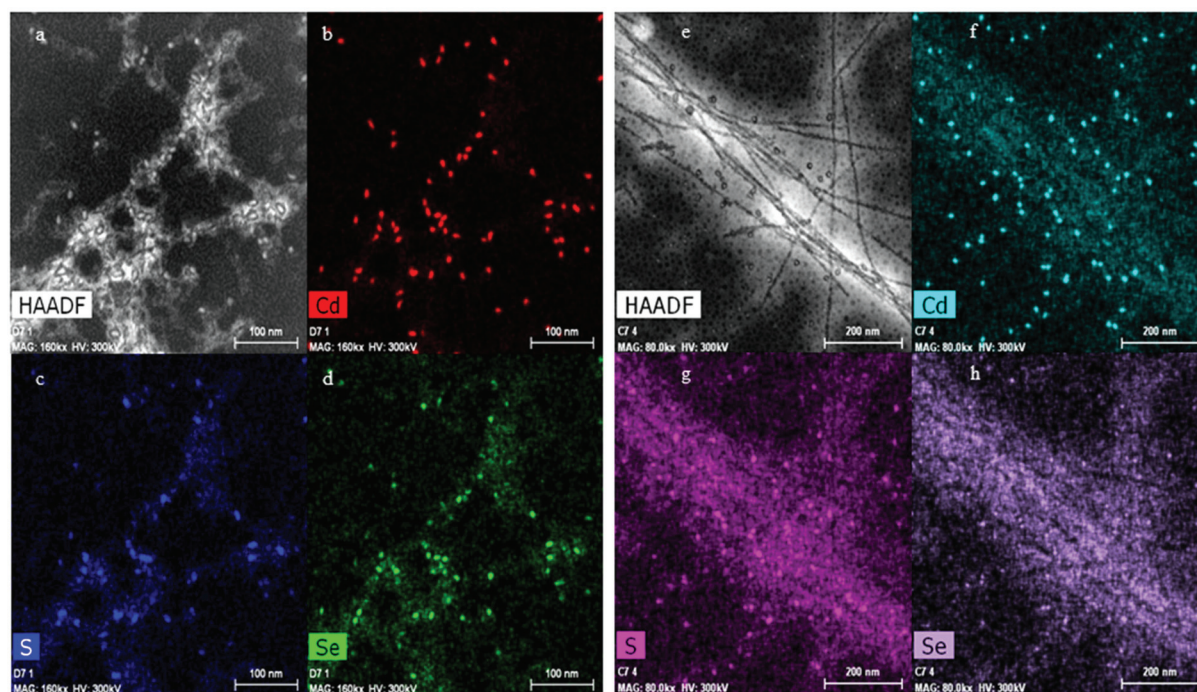
Fig. 8 (a) HAADF-STEM image of QD800 bound to APO protein fibers. (b), (c) and (d) Are the corresponding elemental mapping of Cd, S and Se. (e), (f), (g) and (h) Same for the Blg-QD800 sample.

Blg-globular, which exhibited a τ_D distribution centered at 3.46 ± 0.01 ns. These results demonstrate that in both APO and Blg fibers two different types of structures are formed, which display a more efficient energy transfer and, hence, are more compact than the globular species.

Fluorescent 1D hybrid QD-fibers

Finally, we covalently coupled three types of CdSe nanoparticles (NPs) to APO and Blg fibers for obtaining fluorescent 1D nanostructures. The surface of the QD, covered with free carboxyl (COOH) residues, enables covalent coupling to the QD probes. The conjugation process of fluorescent QDs (525, 655 or 800) emitting at 525, 655 or 800 nm, to 1D fibers of both proteins has been achieved via covalent crosslinking chemistry. Fluorescence emission spectra of APO-QD and Blg-QD fibers (Fig. S5†) showed no significant changes in the emission and bandwidths of QDs after the coupling process to fibers.

The HR-TEM contrasted images of the APO-QD and Blg-QD hybrid nanofibers (Fig. 7) showed that the crosslinking step did not result in fiber aggregation and that the functionalization of fibers with QDs was clearly successful. The semiconductor NPs arrange along the protein nanofibers alternately on either side of the fiber. The organic PEG shell (of about 2 nm) surrounding the QDs could be perfectly distinguished. For the Blg-QD hybrid structures some free QDs in the medium were observed. In the case of APO-QD fibers the functionalization reaction was practically complete and no free QDs were observed in the medium.

The high-angle annular dark-field scanning transmission electron microscopy (HAADF-STEM) images and the energy dispersive X-ray (EDX) analysis of the APO-QDs and Blg-QDs are shown in Fig. 8. The EDX mapping showing colocalization of S, Se and Cd on a single fiber confirms first the presence of the QDs associated with the fibers, and second the successful functionalization.

Conclusions

1D fluorescent nanofibers have been prepared either using apoferritin or β-lactoglobulin proteins as templates. This is the first time that a wire-like, micrometer-sized structure with persistence length formed by the heat treatment of apoferritin is described. Optimizing the heating protocol, which induces the apoferritin protein to denature and self-assemble, allows the formation of 1D fibers. Controlling the experimental conditions such as the temperature, pH and time of incubation used, the morphology and diameter size can be varied. An incubation time of 12 to 24 h, a pH of 2 and 80 °C are the optimal conditions for the formation of wire-like fibers. We showed that apoferritin fibers maintain their ability to be functionalized. Thus, 1D fluorescent fibers with fluorescence emission ranging from green to near-infrared were prepared by coupling dyes or QDs to APO and Blg proteins. FLIM-PIE studies on FRET efficiency within the tagged APO and Blg

fibers demonstrate different arrangements of the proteins in mature fibers than in small aggregates. The arrangement of multiple dye molecules into fiber assemblies exhibits a more efficient energy transfer as compared with their counterpart globular proteins. Moreover, the choice of different donors and acceptors may allow wavelength tunability through intra-fibrillar energy transfer. Therefore, the results demonstrate the chemically versatile nature of this 1D template and its high potential for manufacturing hybrid and functional nanomaterials, specifically fluorescent nanofibers.

The well-established knowledge about the apoferritin structure, the availability of numerous methods for its functionalization and the simplicity of fiber synthesis, makes the APO protein a highly promising template for preparing 1D nanomaterials. The ability to control both, the type and number of fluorophores on a fiber template as opposed to being embedded irregularly in a matrix could be advantageous. This would allow rational manipulation of the energy transfer efficiency by varying the type and number of acceptor and donor fluorophores.

Protein fibrils resulting from the assembly of proteins or peptides into long, highly ordered fibrillar structures are emerging as one of the fastest growing scientific areas, because of their functional versatility and broad applications in biology (amyloid-like fibers are associated with numerous neurodegenerative diseases) and in nanotechnology (as templates for the fabrication of metal nanowires and functional polymer nanotubes). In that sense they can find similar applications as fluorescent organic polymers or inorganic nanowires.

Acknowledgements

Notes and references

1 Z. Tang and N. A. Kotov, Adv. Mater., 2005, 17, 951.
2 M. R. Buck and R. E. Schaak, Angew. Chem., Int. Ed., 2013, 52, 2.
3 M. B. Dickerson, K. H. Sandhage and R. R. Naik, Chem. Rev., 2008, 108, 4935.
4 R. K. Joshia and J. J. Schneider, Chem. Soc. Rev., 2012, 41, 5285.
5 L. Nicole, L. Rozes and C. Sanchez, Adv. Mater., 2010, 22, 3208.
6 S. A. Maier, M. L. Brongersma, P. G. Kik, S. Meltzer, A. A. G. Requicha and H. A. Atwater, Adv. Mater., 2001, 13, 1501.
7 S. A. Maier, P. G. Kik, H. A. Atwater, S. Meltzer, E. Harel, B. E. Koel and A. A. G. Requicha, Nat. Mater., 2003, 2, 229.

8 M. M. Walker, T. E. Dennis and J. L. Kirschvink, *Curr. Opin. Neurobiol.*, 2002, **12**, 735.

9 P. Alivisatos, *Nat. Biotechnol.*, 2004, **22**, 47.

10 B. Pelaz, S. Jaber, D. J. de Aberasturi, V. Wulf, T. Aida, J. M. de la Fuente, J. Feldmann, H. E. Gaub, L. Josephson, C. R. Kagan, N. A. Kotov, L. M. Liz-Marzán, H. Mattoussi, P. Mulvaney, C. B. Murray, A. L. Rogach, P. S. Weiss, I. Willner and W. J. Parak, *ACS Nano*, 2012, **6**, 8468.

11 M. G. Warner and J. E. Hutchison, *Nat. Mater.*, 2003, **2**, 272.

12 M. Masetti, H. Xie, Ž. Krpetić, M. Recanatini, R. a. Alvarez-Puebla and L. Guerrini, *J. Am. Chem. Soc.*, 2015, **14**, 469.

13 J. Pate, F. Zamora, S. M. D. Watson, N. G. Wright, B. R. Horrocks and A. Houlton, *J. Mater. Chem. C*, 2014, **2**, 9265.

14 E. Gazit, *Chem. Soc. Rev.*, 2007, **36**, 1263.

15 X. B. Zhao, F. Pan, H. Xu, M. Yaseen, H. H. Shan, C. A. E. Hauser, S. G. Zhang and J. R. Lu, *Chem. Soc. Rev.*, 2010, **39**, 3480.

16 L. C. Palmer and S. I. Stupp, *Acc. Chem. Res.*, 2008, **41**, 1674.

17 G. Fichman, L. Adler-Abramovich, S. Manohar, I. Mironi-Harpaz, T. Guterman, T. Seliktar, P. Messersmith and E. Gazit, *ACS Nano*, 2014, **8**, 7220–7228.

18 Y. Loo, S. Zhang and A. E. C. Hauser, *Biotechnol. Adv.*, 2012, **30**, 593.

19 D. J. Toft, T. J. Moyer, S. M. Standley, Y. Ruff, A. Ugolkov, S. I. Stupp and V. L. Cryns, *ACS Nano*, 2012, **6**, 7956.

20 T. H. Han, W. J. Lee, D. H. Lee, J. E. Kim, E. Y. Choi and S. O. Kim, *Adv. Mater.*, 2010, **22**, 2060.

21 I. Cherny and E. Gazit, *Angew. Chem., Int. Ed.*, 2008, **47**, 4062.

22 T. Scheibel, R. Parthasarathy, G. Sawicki, X. M. Lin, H. Jaeger and S. L. Lindquist, *Proc. Natl. Acad. Sci. U. S. A.*, 2003, **100**, 4527.

23 X. Zan, S. Feng, E. Balizan, Y. Lin and Q. Wang, *ACS Nano*, 2013, **7**, 8385.

24 A. K. Nair, A. Gautieri, S. W. Chang and M. J. Buehler, *Nat. Commun.*, 2013, **4**, 1724.

25 A. Seidel, O. Liivak, S. Calve, J. Adaska, G. Ji, Z. Yang, D. Grubb, D. B. Zax and L. W. Jelinski, *Macromolecules*, 2000, **33**, 775.

26 S. Keten, Z. Xu, B. Ihle and M. J. Buehler, *Nat. Mater.*, 2010, **9**, 359.

27 Z. Xu, R. Paparcone and M. J. Buehler, *Biophys. J.*, 2010, **98**, 2053.

28 C. Li, A. K. Born, T. Schweizer, M. Zenobi-Wong, M. Cerruti and R. Mezzenga, *Adv. Mater.*, 2014, **26**, 3207.

29 S. J. Eichhorn, A. Dufresne, M. Aranguren, N. E. Marcovich, J. R. Capadona, S. J. Rowan, C. Weder, W. Thielemans, M. Roman, S. Renneckar, W. Gindl, S. Veigel, J. Keckes, H. Yano, K. Abe, M. Nogi, A. N. Nakagaito, A. Mangalam, J. Simonsen, A. S. Benight, A. Bismarck, L. A. Berglund and T. Peijs, *J. Mater. Sci.*, 2010, **45**, 1.

30 T. Nicolai and D. Durand, *Curr. Opin. Colloid Interface Sci.*, 2013, **18**, 249.

31 D. Hamada and C. M. A. Dobson, *Protein Sci.*, 2002, **11**, 2417.

32 C. Li, J. Adamcik and R. Mezzenga, *Nat. Nanotechnol.*, 2012, **7**, 421.

33 S. Bolisetty, J. J. Vallooran, J. Adamcik, S. Handschin, F. Gramm and R. Mezzenga, *J. Colloid Interface Sci.*, 2011, **361**, 90.

34 S. Bolisetty, J. Adamcik, J. Heier and R. Mezzenga, *Adv. Funct. Mater.*, 2012, **22**, 3424.

35 S. Bolisetty, J. J. Vallooran, J. Adamcik and R. Mezzenga, *ACS Nano*, 2013, **7**, 6146.

36 J. M. Jung, G. Savin, M. Pouzot, C. Schmitt and R. Mezzenga, *Biomacromolecules*, 2008, **9**, 2477.

37 G. Jutz, P. van Rijn, B. Santos Miranda and A. Böker, *Chem. Rev.*, 2015, **115**, 1653.

38 B. Fernandez, N. Galvez, P. Sanchez, R. Cuesta, R. Bermejo and J. M. Domınguez-Vera, *J. Biol. Inorg. Chem.*, 2008, **13**, 349.

39 B. Fernandez, N. Galvez, R. Cuesta, A. B. Hungrıa, J. J. Calvino and J. M. Domınguez-Vera, *Adv. Funct. Mater.*, 2008, **18**, 3931.

40 F. Carmona, O. Palacios, N. Galvez, R. Cuesta, S. Atrian, M. Capdevila and J. M. Domınguez-Vera, *Coord. Chem. Rev.*, 2013, **257**, 2752.

41 F. Castello, S. Casares, M. J. Ruedas-Rama and A. Orte, *J. Phys. Chem.*, 2015, **119**, 8260.

42 A. Monserrate, S. Casado and C. Flors, *Chem. Phys. Chem.*, 2014, **15**, 647.